Multi-geophysical approach for characterization of thermally-induced cracks in granite: discussion of repetitivity and durability

Mohmed Salah Boussaid, Céline Mallet, Kévin Beck

▶ **To cite this version:**

Mohmed Salah Boussaid, Céline Mallet, Kévin Beck. Multi-geophysical approach for characterization of thermally-induced cracks in granite: discussion of repetitivity and durability. 2019. hal-02361662v1

HAL Id: hal-02361662

https://hal.science/hal-02361662v1

Preprint submitted on 13 Nov 2019 (v1), last revised 12 Feb 2020 (v2)

HAL is a multi-disciplinary open access archive for the deposit and dissemination of scientific research documents, whether they are published or not. The documents may come from teaching and research institutions in France or abroad, or from public or private research centers.

L'archive ouverte pluridisciplinaire **HAL**, est destinée au dépôt et à la diffusion de documents scientifiques de niveau recherche, publiés ou non, émanant des établissements d'enseignement et de recherche français ou étrangers, des laboratoires publics ou privés.

Distributed under a Creative Commons Attribution - NonCommercial - NoDerivatives 4.0 International License

This work is licensed under a Creative Commons Attribution-NonCommercial-NoDerivatives 4.0 International License.

This is a pre-print of an article submitted to Pure And Applied Geophysics (submission ID PAAG-D-19-00565).

Multi-geophysical approach for characterization of thermally-induced cracks in granite: discussion of repetitivity and durability

Mohmed Salah Boussaid[1], Celine Mallet[1,2], and Kevin Beck[1]

[1]*Université d'Orléans, Université de Tours, INSA Centre Val de Loire - Laboratoire de Mécanique Gabriel Lamé - Polytech Orléans, 8 rue Léonard de Vinci, 45072 Orléans, France*
[2]*Univ. Orléans, CNRS, BRGM, ISTO, UMR 7327, F-45071, Orléans, France*

Abstract In this work, we propose an experimental study to characterize micro-scale damage introduced in a granite with two different thermal treatments performed at low temperature: the slow cooling and the thermal shock. Damage is characterized by monitoring of elastic wave velocity and thermal conductivity. The same protocol is performed on 5 samples in order to discuss the repetitivity of the induced damage. It is observed that the thermal shock protocol leads to a more pronounced damage interpreted in terms of a larger variety of nucleated intragranular and intergranular cracks, that were observed by microscopes. However, this more important damage seems not to be repetitive from one sample to another compared to the damage introduced by slow cooling. Following this first result, a time follow-up for wave velocity, conductivity and mercury porosity is proposed. It appears that the damage introduced by the slow cooling, unlike the thermal shock, does not present a long durability. After 15 days, the different properties had returned to their initial state. A time-dependence mechanism is proposed to discuss this observed process.

Keywords
cracks
thermal treatment
granite
elastic wave velocity
microscopic observations
thermal conductivity
porosity

Introduction

For both engineering and geological applications, it is of great importance to further our knowledge about thermally-induced cracks in rocks. Studying the thermally induced crack is of direct and various applications [Kranz, 1983]. Indeed, it is common that rock undergoes heating and cooling processes of different degrees in several fields, including the development and use of geothermal energy, the storage of radioactive waste in geological formations and the oil field development [Ringwood, 1985; Cappa and Rutqvist, 2011; Feng et al, 2012; Nakaten et al, 2014]. For these applications, the characterization and prediction of the evolution of the crack network when rocks undergo thermal variations is of major interest.

Especially, Enhanced Geothermal Systems consist of improve an existing cracked areas in order to use the local permeability to transport hot fluids. Several geothermal reservoirs are studied in Granite formation as for the French site of Soultz-sous-Foret [Rummel, 1992]. Thus, in the literature, there are many studies that emphasize the influence of thermally induced cracks on different granite physical behavior. In particular, it has been noted that cracking and changes in elastic properties are associated with changes in elastic wave velocities [Lin, 2002; Nasseri et al, 2007; Chaki et al, 2008; Griffiths et al, 2017; Zhang et al, 2018]. It has been shown that the two parameters, temperature and wave velocity, are inversely correlated and that induced microstructural damage has a significant effect on wave velocity [Hadley, 1976]. Other studies also focus on the variation in the physical properties of granite subjected to thermal stresses, particularly in relation with porosity [David et al, 1999; Chen et al, 2017] and thermal properties as thermal conductivity [Dwivedi et al, 2008; Kant et al, 2017; Zhao et al, 2018]. They showed that thermal conductivity of a cracked granite tends to decrease as temperature increases and thermally induced cracking occurs. Other studies demonstrate the effect of thermal shocks to induce cracks on the physical and mechanical behavior of granite [Kim et al, 2014; Kumari et al, 2017; Jin et al, 2019].

In the laboratory, there are different thermal protocols used to understand how cracks are nucleated in geothermal conditions. They differ by heating rates, maximal temperature, cooling rate and number of cycles. It has been shown that cooling rate and maximal temperature are often a key parameter to control the crack network [Belayachi et al, 2019]. In our study, two cooling protocols are considered: slow cooling [Wang et al, 2013] and thermal shocks [Ougier-Simonin et al, 2011; Mallet et al, 2015], both at different degree of maximal temperature [Beck et al, 2016]. About the temperature range, in the literature it is common to find studies investigating the thermally induced cracks at temperatures from 200^{o}C to 600^{o}C [Zhao et al, 2017; Rong et al, 2018; Gautam et al, 2018]. However, in the field, thermal ranges are not always extremely high, especially in shallow reservoirs. Consequently, it is of great interest to study the range of 100-200^{o}C for conventional geothermal projects [Rummel, 1992]. In addition, at these temperatures, micro-cracks may still occurs. Indeed, it has been shown that cracks may started to nucleate at a temperature of 75^{o}C [Richter and Simmons, 1974]. Our

Table 1 The considered granite compared to La Peyratte and Westerly granites.

	This granite	La Peyratte	Westerly
Composition	40% quartz,	28,5% quartz,	27% quartz,
	13% feldspar	20% feldspar	36% feldspar
	14% plagioclase,	38,5% plagioclase,	30% plagioclase,
	24% biotite,	8% biotite,	6% biotite,
	9% muscovite	5% muscovite	1% accessories
Grain size	200-300 μm	200 μm	500 μm
Porosity	1.4%	$<$1%	1%
Reference	this study	[Wang et al, 2013]	[Spray, 2010; Wang et al, 2012]

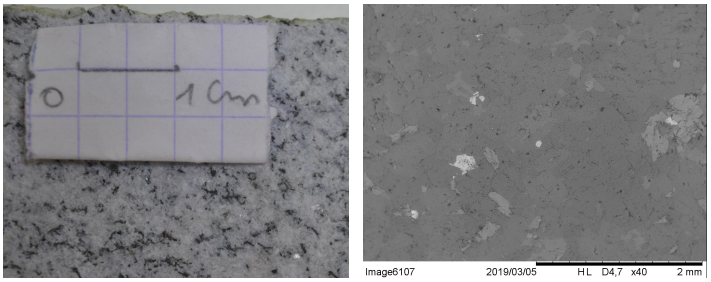

Figure 1 Picture and microscopic view by Scanning Electron Microscopy (x40) of the used granite in this study.

study aims at investigating the thermally induced cracks under this temperatures through a geophysical characterization of their density, connectivity and time-durability.

To do so, a multi-geophysical approach is proposed [Zhao et al, 2017]. Crack density will be characterized through elastic wave velocity measurements (see the recent review of Guéguen and Kachanov [2011]). The connectivity of the crack network will be discussed through thermal conductivity [Xiong and Liew, 2016; Wuttke et al, 2017] and mercury porosity measurements. Finally, the crack geometry will be illustrated by SEM pictures.

This presented paper aims at answering three issues in the context of cracked-enhanced geothermal reservoir in granite. First of all, we want to quantify the thermally induced crack network in granite submitted to low temperatures and compare the effect of slow and instantaneous coolings on the crack network. Then, it is expected to improve our knowledge on coupled multi-geophyscal approach to characterize cracks from external non-destructive approaches. These tools being always in the need of a better development to obtain coupled information and improve the resolutions [Ndao et al, 2017]. Finally and from a more general point of view, we would like to discuss the repetitive and durable aspects of such thermally-induced crack networks. Indeed, many of researchers carry out thermal treatments to prepare cracked samples. This last point answer a common issue encountered here: is the result of these treatments the same from one sample to another? and after few days, is it still constant ? It will be investigated with observations performed on various samples and with a time follow-up during 15 days. These questions will not be totally answered but this paper represents a first contribution to it at least for treatments at low temperatures.

1 Methodology and theoretical context

1.1 Samples

The samples used in this study are fine-grained granite that presents an average grain size of 200-300 μm with an initial porosity of 1.4%. The initial P and S wave velocities are about 4070 and 2560 m/s, respectively. The initial thermal conductivity has been found at 2,35 W/m.K $\pm$ 0.09. Its modal composition is compared to Westerly granite and La Peyratte granite (Table 1 and Figure 1).

A total of 27 prismatic samples of 3x3x6 cm, were prepared and submitted to two thermal protocols in order to characterize the initial state, investigate the repetitive aspect of the thermally induced crack networks and follow the damage evolution with time (Table 2).

1.2 Thermal treatments

Two thermal treatments are considered. They differ by their cooling path. For both treatments, the used oven has a maximal temperature of 200^{o}C with an accuracy of 0.1^{o}C. This oven can be regulated in order to program automatic cycles. The temperature paths are as follow: temperature is increased up to a maximal temperature at a rate of 1^{o}C/min in order to avoid any dynamic damage during the heating [Ougier-Simonin et al, 2011; Mallet et al, 2013]. Samples are maintained at this level during at least 6 h to ensure a complete temperature diffusion within the sample core (recently discussed

Table 2 Samples, thermal treatments and measured properties. EWV stands for Elastic Wave Velocity

Samples	Thermal treatment	Measurements
1 to 5	PC	EWV, thermal conductivity, EWV at day 15
6 to 10	TS	EWV, thermal conductivity, EWV at day 15
11 to 12	PC	EWV and thermal conductivity during 12 days
13 to 27	PC	Porosity at initial state and during 12 days (smaller samples)

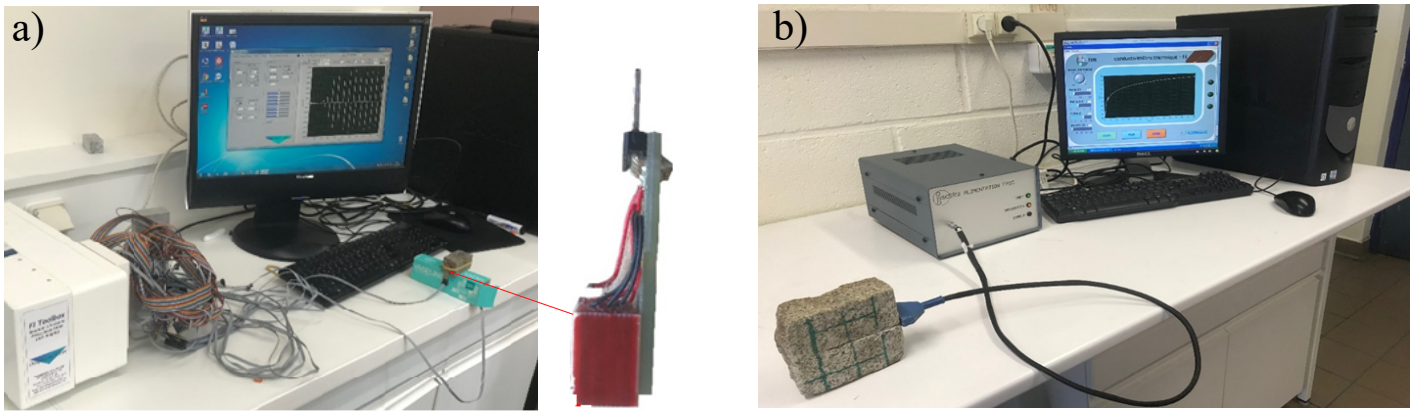

Figure 2 Pictures of our sensors for geophysical analyses: a) Piezoelectric sensor and its device. b) Thermal conductivity set-up.

by Zhang et al [2018]). Then, for the first thermal treatment, samples are cooled down at 1^{o}C/min. This treatment will be referred as progressive cooling (PC). For the second treatment, samples are quenched in a few second into water at ambient temperature. This treatment will be referred as thermal shock (TS).

These thermal treatments are successively performed at 100^{o}C, 150^{o}C and 180^{o}C.

Physical properties are measured after 6 h of full cooling. Table 2 presents a summary of the 27 samples with the corresponding thermal treatments and measurements.

1.3 Physical measurements

Porosity measurements have been performed thanks to a mercury porosimeter on smaller cylindric samples of 1 cm-diameter and 2 cm-length, taken from the prismatic samples. Microstructural observations are obtained by scanning electron microscope (SEM) and optical microscope. Then, the geophysical characterization is based on two measurements, the elastic wave velocity and the thermal conductivity. We detail below these two measurements together with their considered theoretical interpretations.

1.3.1 Elastic wave velocity and crack density

Elastic wave velocities were measured with piezoelectric sensors (PI Ceramic) put directly on the sample surface (Figure 2a). Honey was used as coupling gel to ensure a good contact [Ndao et al, 2017]. Two sensors were put on opposite longest faces of the sample in order to avoid noise. Then, an electric pulse of 150 V is generated and transmitted to the first sensor. It triggers a mechanical vibration that propagates into the sample at a frequency of 1 MHz. The opposite sensor records this vibration and transforms it into an electrical signal that is amplified at 30 dB. A dedicated interface allows to observe the recorded waveform. Finally, the travel time is manually picked. The wave velocity is deduced knowing the distance between the two sensors [Birch, 1960]. Sensors are sensitive to compressional (P) waves. They are determined with an accuracy of $\pm$50 m/s. The velocity decrease will be interpreted in terms of increasing crack density [Walsh, 1965].

1.3.2 Thermal conductivity and crack connectivity

For the characterization of crack's transport properties, elastic wave velocities are not enough. Due to their inversion, they only describe the global amount of cracks. Thus, two crack networks can have the same crack density and totally different shape [Mallet et al, 2013], degree of connectivity [Caspari et al, 2016], and thus transport properties. In order to go further in the crack network characterization, a measurement that indicates the crack connectivity is needed. It is in this idea that we measured the thermal conductivity. This measurement is actually an effective thermal conductivity. Indeed our sample can be locally considered as heterogeneous. However, for sake of simplicity, and because grains are small and homogeneous in our granite, we keep the term of thermal conductivity.

As shown by Xiong and Liew [2016], thermal or electrical conductivities are linked to the connectivity of a crack network. For the thermal effects, when a sample is more porous, its thermal conductivity decreases. With connectivity of cracks, this phenomenon is enhanced. Our measurement was performed by the hotwire technique (Figure 2b) following ASTM D5930-97 and the RILEM recommendations (AAC11-3). The Neotim apparatus used is equipped with a probe of 50 mm-length. The accuracy of the measurement is $\pm$5% with a repeat accuracy of 3%. The temperature range of the apparatus is from

-20^{o}C to 100^{o}C. The measurement range of thermal conductivity is 0.02-5 W/mK. For every measurement, the average conductivity was obtained from 10 measurements in order to minimize the standard deviation.

2 Results

2.1 Thermally-induced damages

2.1.1 Elastic-wave velocity

After each thermal treatment at 100^{o}C, 150^{o}C and 180^{o}C, for the PC and TS, P-wave velocity is measured (Figure 3) in order to follow the progressive damage introduced in the samples. Here, the ten first samples are used (see Table 2). Samples 1 to 5 for the PC, with circle, square,bobin, triangle and star as their respective empty symbol ; and five for the TS, with plain circle, square, bobin, triangle and star as their respective symbol. The average value obtained at each temperature is highlighted with blue dots.

After the successive PC a global decrease of P-wave velocity is noticed until 150^{o}C followed by a slight increase of 50 m/s at 180^{o}C. Despite this re-increase, between the initial and final state, a damage of the sample is obtained with an average velocity decrease of 275 m/s. The homogeneity between each sample is relatively correct and one could said that the damage introduced by this thermal protocol can be reproduced in terms of elastic wave velocity variation. Indeed, there is a discrepancy of $\pm$100 m/s that is constant when damage increases (from 100^{o}C).

After the TS, a global velocity decrease is also observed without the local re-increase around 150^{o}C (except for one sample). Between the initial state and the final one, the damage of the sample is characterized by a velocity decrease of 575 m/s. However, this damage presents a larger discrepancy between the five samples of $\pm$350 m/s. Looking at this data, it is not possible, according to us, to conclude about a correct repetitivity of this damage protocol.

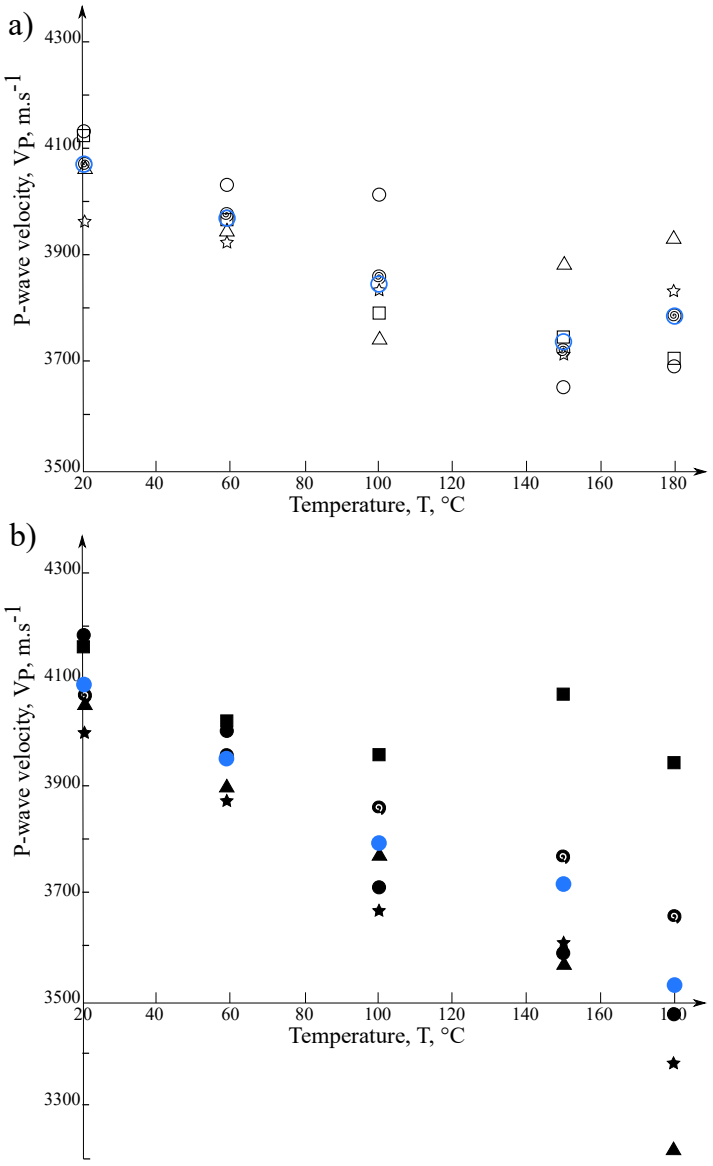

Figure 3 P-wave velocities measured after the thermal treatments for the progressive cooling (a) and the thermal shock (b). The different symbols represent the different samples (see Table 2). The blue dots are the average value at each temperature.

2.1.2 Thermal conductivity

Thermal conductivity is presented on Figure 4 for the PC (a) and the TS (b). Because the measurementcannot be done on a single sample but at the interface of two samples, the symbology of Figure 3 is not used here. Instead, the obtained average value and the discrepancy is plotted

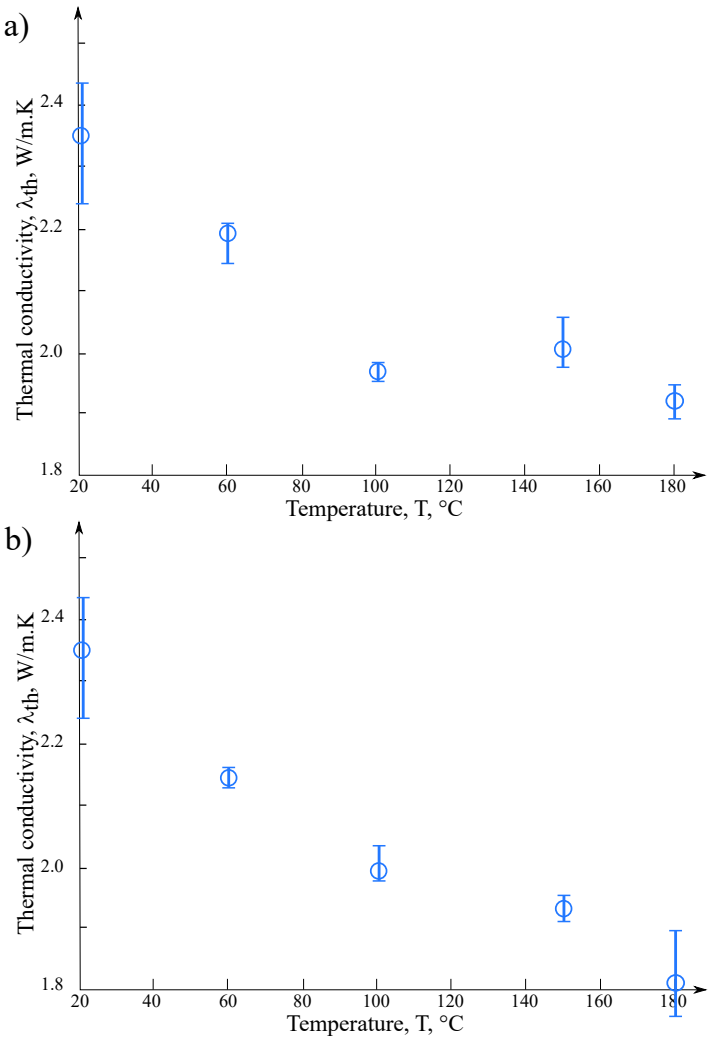

Figure 4 Thermal conductivity measured after the thermal treatments for the progressive cooling (a) and the thermal shock (b). The main value is plotted with the measured discrepancy as error bars.

For the PC, the same behavior is observed with thermal conductivity as with the P-wave velocity: a decrease highlighting the damage of the sample from 2.35 to 1.98 W/m.K. Then, a rebound of 0.2 W/m.K around 150^{o}C, followed by a final decrease. This rebound is discussable with respect to the discrepancy of the results. Even so, the global decrease is interrupted.

For the TS, the global decrease is continuous and reach a lower value of 1.8 W/m.K. At the highest damage level, the discrepancy of the result is less accurate.

As a summary, whatever the measurement, for the TS, damage increases with the temperature without singularity and the repetitivity between the samples is less and less good as the damage increases. For the PC, damage appears to be less important, the repetitivity is much better and a singularity appears around 150^{o}C that will be discussed below in section 3.

2.2 Damage durability

In order to discuss the durability of the induced damage, elastic wave velocities were re-measured after 15 days. The results are reported on Figure 5. It appears that the damage introduced by the PC after 180^{o}C returns to its initial value after 15 days. The damage introduced by the TS is slightly reduced but remains present and non-negligible.

In order to better describe this evolution, P-wave velocity, thermal conductivity and Hg-porosity have been measured on new samples (see Table 2) between 2 and 15 days after the full protocol of PC. Results are presented on Figure 6. In this figure, points at day 0 represent the initial state while points at day 1 represent the properties measured just after the complete cooling of the samples after the treatment.

After their decrease, the P-wave velocity is constant during 5 days. After the first five days, it started to increase. The initial state is recovered after 11 days. The thermal conductivity has a similar trend but slower: this measurement is

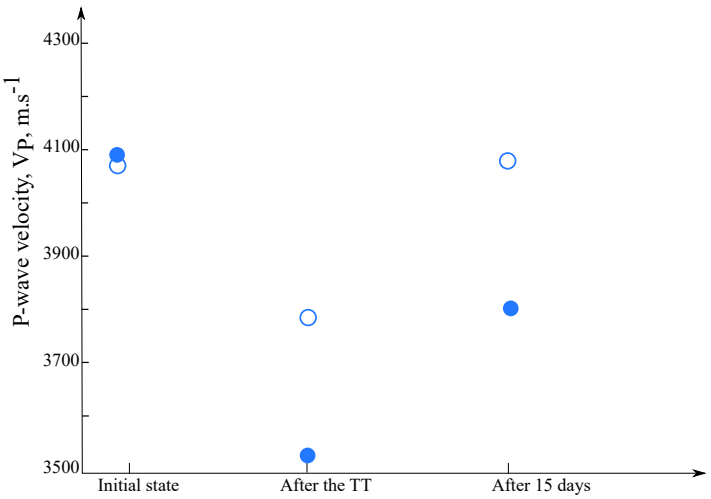

Figure 5 P-wave velocities at initial state, measured after the thermal treatments for the PC (empty circles) and the TS (plain circles), and after 15 days.

almost constant up to 7 days, and after 15 days, 87% of the initial state is recovered. The measurement of the porosity presents the same behavior at an intermediate rate between the P-wave velocity and thermal conductivity variations. Note that there is a very large discrepancy at day 2. This value will not be considered. Without it, the damage introduced by the PC increased the porosity from 1,4 to 2%. It remains constant during 5 days as the P-wave velocity and the thermal conductivity and then started to decrease but slower than the P-waves. After 15 days the initial state is not recovered as for the thermal conductivity.

3 Discussion

3.1 Slow cooling versus thermal shocks

Looking at both treatments, it appears that besides the low involved temperature, a real damage is introduced in the samples. From the literature, we know that there are two ways to thermally initiate cracks. On one hand, cracks may be induced when the temperature homogeneously and gradually changes. It causes a favored expansion of some minerals over the others due to the difference in associated thermal expansion coefficients [Friedman et al, 1978; Bauer et al, 1979]. On the other hand, cracks may be initiated due to a sudden change in temperature leading to very high local stresses [Jansen et al, 1993]. These differences of behavior could explain the differences observed between our two protocols. These observations have also been previously described by Jin et al [2019]. In this previous study, the authors concluded that the stresses from the thermal shock have a greater effect on the rock than those from the progressive cooling. Looking at our results, this previous observation is confirmed: thermal shocks lead to a much more important damage of the sample. This result is quite intuitive when thinking of the brutality of the involved stresses [Ougier-Simonin et al, 2011]. Note, however, that opposite trend has been observed on different sandstones [Belayachi et al, 2019] highlighting the importance of the mineral composition and initial porosity.

To understand where does come from the more important crack network induced by the TS, we performed some observations at optical microscope and SEM (Fig 7). We observed large cracks developed at the sample boundaries (Fig 7b), together with cracks developing around (Fig 7c-d) and inside grains (Fig 7e-f) in the samples submitted to TS but not on PC where only diffuse cracks were observed with a need of a larger magnification (Fig 7g-h). These two crack families are referred as intergranular (Fig 7c-d) versus intragranular (Fig 7e-f) cracks in the literature [Nasseri et al, 2009].

3.2 Singularity in damage induced by the PC

During the damage evolution of samples submitted to PC, a singularity appears around 150^{o}C. Locally, the P-wave velocities and the thermal conductivity present a rebound in their progressive decreases. We interpret this singularity by the competition between two microstructural behaviors. Similar singularities can be found in the literature also interpreted in terms of dual behavior competition [Darot et al, 1992]. In this study, the authors observed a permeability decrease with damage around temperatures of 150^{o}C. They interpreted this permeability decrease by the low mineral expansion that is supposed to cause thermally induced microcracks and permeability increase. This expansion would have been so low that joins dilatation would have been accommodated by cracks, leading to a channel closure. In our case, a similar dual competition can be described.

On one side, around the range of 150^{o}C a mineral dilatation is expected under the thermal effects [Cooper and Simmons, 1977; Wong and Brace, 1979]. This dilatation leads to a closure of pores and pre-existing cracks [Bachrach et al, 2000]. This closure will lead to a wave velocity and thermal conductivity increases.

On the other side, according to Lin [2002], the thermal threshold for crack initiation in granite is around 100-125^{o}C. A lower threshold can be found also in the literature (around 75^{o}C according to Richter and Simmons [1974]). This threshold is the competitor process forcing the wave velocity and thermal conductivity to decrease.

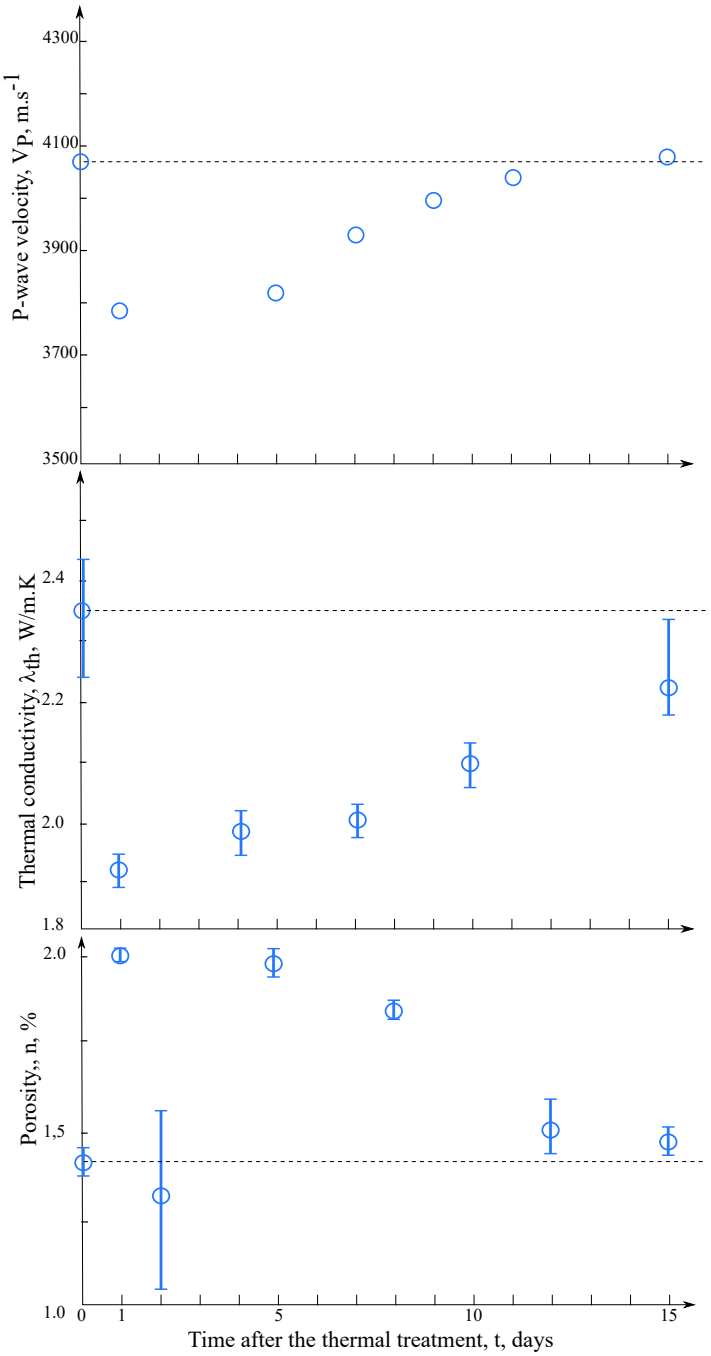

Figure 6 P-wave velocities, thermal conductivity and porosity at the initial state (day 0), after the thermal treatment of PC (day 1) and during 15 days. Initial state are highlighted with dashed lines.

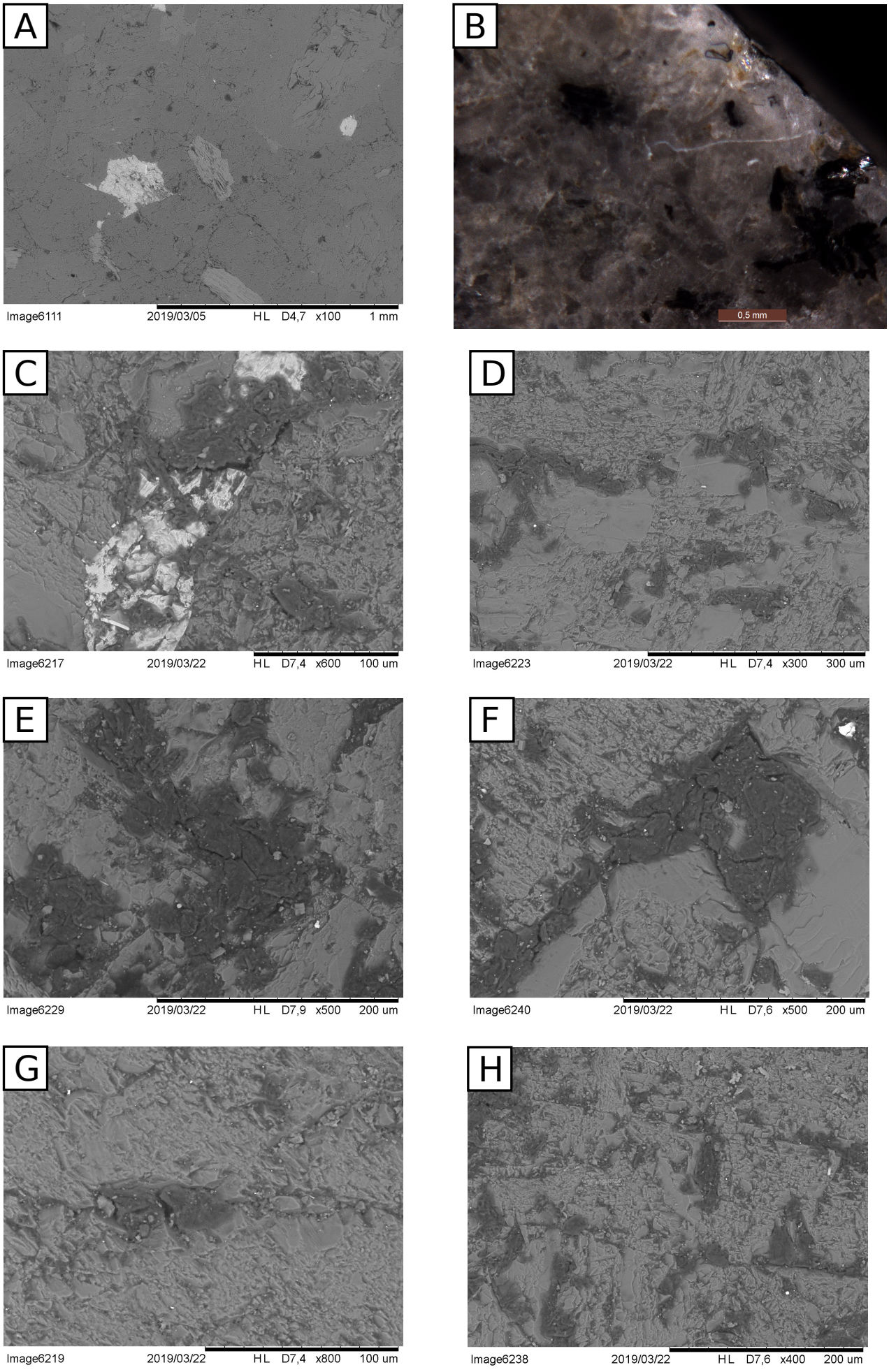

Figure 7 Microstructural observations in our cracked samples. a) Initial state with well closed joins. b) - f) Observations made on samples after the TS protocols: b) from optical microscope, on the sample boundary and c) - f) from SEM. g) - h) Observations made on samples after the PC protocols with SEM.

3.3 Crack's closure with time, after the PC

After the PC, damage have been introduced. It has been highlighted by wave velocity and thermal conductivity decreases. It has been interpreted in terms of cracking. They have been observed with the SEM. But, these cracks return to their initial state after almost 15 days. Successively, the P-wave velocity, then the porosity and thermal conductivity returns to their initial values. We would like here, to discuss a possible interpretation.

P-wave sensors have a central frequency of 1 MHz thus a wavelength of 4 mm. They are thus mostly sensitive to cracks of 0,1 mm-size. Hg-porosity is sensitive to all cracks and pore. Thermal conductivity is sensitive to surface cracks, as spalling [Al-Omari et al, 2016], especially in our case with the hot-wire apparatus.

Looking at the time evolution of these three parameters (first the P-wave velocity, then the porosity, finally the thermal conductivity) we propose the following mechanism : at the beginning, and because of pressure equilibrium starting at the sample core, inner cracks started to close. It leads to a P-wave velocity and porosity re-increase. Progressively, all cracks, up to those of the surface will close. But because of the use of coupling gel, P-wave are not sensitive to the surface spalling and thus, they return to their initial state before the spalling is closed and while the porosity and thermal conductivity are not yet returned to their initial states.

The time-dependent variation of cracks due to a constant pressure has been discussed in the literature [Mallet et al, 2015; Laubach et al, 2019]. According to Lawn and Wilshaw [1975] and Darot and Gueguen [1986], there is an energy threshold (the activation energy) between two positions x and $x \pm dx$ for a crack elementary propagation or closure that can be described with an exponential law:

$$\frac{dl}{dt}^{+} = \dot{l_0} e^{\frac{-(E_a - \delta E_a)}{kT}} \qquad \frac{dl}{dt}^{-} = \dot{l_0} e^{\frac{-(E_a + \delta E_a)}{kT}} \tag{1}$$

where dl/dt is the crack length velocity, E_a is the activation energy and δE_a is the added energy to overpass the threshold of crack closure (left) or propagation (right). In most of the case, involved stress tends to propagate the cracks and the second equation is predominant [Mallet et al, 2015]. However, in our case the reduction of thermal stresses could be interpreted in terms of the first case leading to an exponential time-dependent crack closure. When looking at Figure 6a, P-wave velocities (having the same variation as crack density and so crack length) return to the initial state with a law that could be described by an exponential, with a correlation coefficient of 0,96.

4 Conclusion

Two thermal treatments at low temperature (up to 180^{o}C) has been performed on granite samples. A progressive one and a shock. Damage has been follow during the successive treatments and during 15 days by P-wave velocity and thermal conductivity. Porosity has been added for the time follow-up. After the thermal treatments microscopic observations have been done thanks to SEM and optical microscope.

It appears that

1. Thermal shock induces an important damage even so the considered temperatures are low. It is characterized by surface cracks but also cracks developing inside and around grains (intergranular and intragranular cracks). This protocol seems to be efficient to introduce cracks. Besides, from one sample to another, the induced damages are not the same. This issue is quite problematic when thinking of all the studies using such protocol for preparing their cracked samples (see the references cited in the introduction). It is perhaps due to the level of damage that needs to be more important. This question will be the target of a future contribution.

2. Progressive cooling brings a lower damage nevertheless observed with SEM. Indeed, diffuse cracks in the matrix has been noted. This damage is, however, reproducible from one sample to another.

3. With the progressive cooling, a singularity has been observed around 150^{o}C. It is interpreted in terms of a competition between grain dilatation that tends to close the pre-existing cracks and the pores, and the development of new cracks.

4. With time, the damage induced by the progressive cooling closes. It seems that it follows a time-dependent exponential law that could explain the process of stress equilibrium with time.

5. Our multi-geophysical approach shows the interest of considering various measurements for coupled interpretations. They highlight different crack behaviors.

Acknowledgements Data reported in this work can be obtained from the corresponding author (Céline Mallet) upon request. Financial support from Lamé Laboratory is gratefully acknowledged by the authors.

References

Al-Omari A, Brunetaud X, Beck K, Al-Mukhtar M (2016) Hygrothermal stress and damage risk in the stones of the castle of chambord-france. International Journal of Civil and Structural Engineering 4(3):doi:10.6088/ijcser.201304010039 *(Cited page 9)*

Bachrach R, Dvorkin J, Nur AM (2000) Seismic velocities and poisson's ratio of shallow unconsolidated sandsseismic properties of shallow sands. Geophysics 65(2):559–564 *(Cited page 6)*

Bauer S, Johnson B, et al (1979) Effects of slow uniform heating on the physical properties of the westerly and charcoal granites. In: 20th US symposium on rock mechanics (USRMS), American Rock Mechanics Association *(Cited page 6)*

Beck K, Janvier-Badosa S, Brunetaud X, Torok A, Al-Mukhtar M (2016) Non-destructive diagnosis by colorimetry of building stone subjected to high temperatures. European Journal of Environmental and Civil Engineering 20(6):643-655 *(Cited page 1)*

Belayachi N, Mallet C, El Marzak M (2019) Thermally-induced cracks and their effects on natural and industrial geomaterials. Journal of Building Engineering 25:100806 *(Cited pages 1 and 6)*

Birch F (1960) The velocity of compressional waves in rocks to 10 kilobars, part 1. Journal of Applied Mechanics 65:1083–1102 *(Cited page 3)*

Cappa F, Rutqvist J (2011) Modeling of coupled deformation and permeability evolution during fault reactivation induced by deep underground injection of co2. International Journal of Greenhouse Gas Control 5(2):336–346 *(Cited page 1)*

Caspari E, Milani M, Rubino JG, Muller TM, Quintal B, Holliger K (2016) Numerical upscaling of frequency-dependent p-and s-wave moduli in fractured porous media. Geophysical Prospecting 64(4):1166–1179 *(Cited page 3)*

Chaki S, Takarli M, Agbodjan W (2008) Influence of thermal damage on physical properties of a granite rock: porosity, permeability and ultrasonic wave evolutions. Construction and Building Materials 22(7):1456–1461 *(Cited page 1)*

Chen S, Yang C, Wang G (2017) Evolution of thermal damage and permeability of beishan granite. Applied Thermal Engineering 110:1533–1542 *(Cited page 1)*

Cooper H, Simmons G (1977) The effect of cracks on the thermal expansion of rocks. Earth and Planetary Science Letters 36:404–412 *(Cited page 6)*

Darot M, Gueguen Y (1986) Slow crack growth in minerals and rocks: Theory and experiments. Pure and Applied Geophysics 124(4):677–692 *(Cited page 9)*

Darot M, Gueguen Y, Baratin M (1992) Permeability of thermally cracked granite. Geophysical Research Letter 19(9):869–872 *(Cited page 6)*

David C, Menéndez B, Darot M (1999) Influence of stress-induced and thermal cracking on physical properties and microstructure of la peyratte granite. International Journal of Rock Mechanics and Mining Sciences 36(4):433–448 *(Cited page 1)*

Dwivedi R, Goel R, Prasad V, Sinha A (2008) Thermo-mechanical properties of indian and other granites. International Journal of Rock mechanics and mining Sciences 45(3):303–315 *(Cited page 1)*

Feng Z, Zhao Y, Zhou A, Zhang N (2012) Development program of hot dry rock geothermal resource in the yangbajing basin of china. Renewable energy 39(1):490–495 *(Cited page 1)*

Friedman M, Johnson B, et al (1978) Thermal cracks in unconfined sioux quartzite. In: 19th US Symposium on Rock Mechanics (USRMS), American Rock Mechanics Association *(Cited page 6)*

Gautam P, Verma A, Jha M, Sharma P, Singh T (2018) Effect of high temperature on physical and mechanical properties of jalore granite. Journal of Applied Geophysics 159:460–474 *(Cited page 1)*

Griffiths L, Heap M, Baud P, Schmittbuhl J (2017) Quantification of microcrack characteristics and implications for stiffness and strength of granite. International Journal of Rock Mechanics and Mining Sciences 100:138–150 *(Cited page 1)*

Guéguen Y, Kachanov M (2011) Effective elastic properties of cracked rocks - an overview, in, mechanics of crustal rocks. CISM Courses and Lectures 533:73–125 *(Cited page 2)*

Hadley K (1976) Comparison of calculated and observed crack densities and seismic velocities in westerly granite. Journal of Geophysical Research 81(20):3484–3494 *(Cited page 1)*

Jansen D, Carlson S, Young R, Hutchins D (1993) Ultrasonic imaging and acoustic emission monitoring of thermally induced microcracks in lac du bonnet granite. Journal of Geophysical Research: Solid Earth 98(B12):22231–22243 *(Cited page 6)*

Jin P, Hu Y, Shao J, Zhao G, Zhu X, Li C (2019) Influence of different thermal cycling treatments on the physical, mechanical and transport properties of granite. Geothermics 78:118–128 *(Cited pages 1 and 6)*

Kant MA, Meier T, Rossi E, Schuler M, Becker D, Höser D, Rudolf von Rohr P (2017) Thermal spallation drilling-an alternative drilling technology for hard rock drilling. Oil Gas 3(1):OG23–OG25 *(Cited page 1)*

Kim K, Kemeny J, Nickerson M (2014) Effect of rapid thermal cooling on mechanical rock properties. Rock mechanics and rock engineering 47(6):2005–2019 *(Cited page 1)*

Kranz RL (1983) Microcracks in rocks: a review. Tectonophysics 100(1-3):449–480 *(Cited page 1)*

Kumari W, Ranjith P, Perera M, Chen B, Abdulagatov I (2017) Temperature-dependent mechanical behaviour of australian strathbogie granite with different cooling treatments. Engineering geology 229:31–44 *(Cited page 1)*

Laubach SE, Lander RH, Criscenti LJ, Anovitz LM, Urai JL, Pollyea RM, Hooker JN, Narr W, Evans MA, Kerisit SN (2017) The Role of Chemistry in Fracture Pattern Development and Opportunities to Advance Interpretations of Geological Materials. Reviews of Geophysics 57 doi:10.1029/2019RG000671 *(Cited page 9)*

Lawn B, Wilshaw R (1975) Fracture of brittle solids. Cambridge university press *(Cited page 9)*

Lin W (2002) Permanent strain of thermal expansion and thermally induced microcracking in inada granite. Journal of Geophysical Research: Solid Earth 107(B10):ECV–3 *(Cited pages 1 and 6)*

Mallet C, Fortin J, Guéguen Y, Bouyer F (2013) Effective elastic properties of cracked solids: an experimental investigation. International Journal of Fracture 182(2):doi: 10.1007/s10704–013–9855–y *(Cited pages 2 and 3)*

Mallet C, Fortin J, Guéguen Y, Bouyer F (2015) Brittle creep and subcritical crack propagation in glass submitted to triaxial conditions. Journal of Geophysical Research 120(2):879–893, doi: 10.1002/2014JB011231 *(Cited pages 1 and 9)*

Nakaten N, Schlüter R, Azzam R, Kempka T (2014) Development of a techno-economic model for dynamic calculation of cost of electricity, energy demand and co2 emissions of an integrated ucg–ccs process. Energy 66:779–790 *(Cited page 1)*

Nasseri M, Schubnel A, Young R (2007) Coupled evolutions of fracture toughness and elastic wave velocities at high crack density in thermally treated westerly granite. International Journal of Rock Mechanics and Mining Sciences 44(4):601–616 *(Cited page 1)*

Nasseri M, Schubnel A, Benson PM, Young R (2009) Common evolution of mechanical and transport properties in thermally cracked westerly granite at elevated hydrostatic pressure. Rock Physics and Natural Hazards 166:5–7 *(Cited page 6)*

Ndao B, Do DP, Hoxha D (2017) P and s wave anisotropy to characterize and quantify damage in media: laboratory experiment using synthetic sample with aligned microcracks. Geophysical Prospecting 65:181–200 *(Cited pages 2 and 3)*

Ougier-Simonin A, Guéguen Y, Fortin J, Schubnel A, Bouyer F (2011) Permeability and elastic properties of cracked glass under pressure. Journal of Geophysical Research 116:B07203, doi:10.1029/2010JB008077 *(Cited pages 1, 2, and 6)*

Richter D, Simmons G (1974) Thermal expansion behavior of igneous rocks. In: International Journal of Rock Mechanics and Mining Sciences & Geomechanics Abstracts, Elsevier, vol 11, pp 403–411 *(Cited pages 1 and 6)*

Ringwood A (1985) Disposal of high-level nuclear wastes: a geological perspective. Mineralogical magazine 49(351):159–176 *(Cited page 1)*

Rong G, Peng J, Cai M, Yao M, Zhou C, Sha S (2018) Experimental investigation of thermal cycling effect on physical and mechanical properties of bedrocks in geothermal fields. Applied Thermal Engineering 141:174–185 *(Cited page 1)*

Rummel F (1992) Physical properties of the rock in the granitic section of borehole gpk1, soultz-sous-forêts. Geothermal Energy in Europe: the soultz hot dry rock project pp 199–216 *(Cited page 1)*

Sarout J (2006) Propriétés physiques et anisotropie des roches argileuses: Modélisation micromécanique et expériences triaxiales. PhD thesis *(Not cited)*

Spray J (2010) Frictional melting processes in planetary materials: From hypervelocity impact to earthquakes. Annual Review of Earth and Planetary Sciences 38:221–254 *(Cited page 2)*

Walsh J (1965) The effect of cracks on the uniaxial elastic compression of rocks. Journal of Geophysical Research 70(2):399–411 *(Cited page 3)*

Wang X, Schubnel A, Fortin J, Gueguen Y, Ge HK (2012) High Vp/Vs ratio: Saturated cracks or anisotropy effects? Geophysical Research Letters 39:L11307, doi:10.1029/2012GL051742 *(Cited page 2)*

Wang X, Schubnel A, Fortin J, Gueguen Y, Ge HK (2013) Physical properties and brittle strength of thermally cracked granite under confinement. Journal of Geophysical Research 118:6099–6112, doi: 10.1002/2013JB010340 *(Cited pages 1 and 2)*

Wong T, Brace W (1979) Thermal expansion of rocks: Some measurements at high pressure. Tectonophysics 57:95–117 *(Cited page 6)*

Wuttke F, Sattari A, Rizvi Z, Motra H (2017) Advanced meso-scale modelling to study the effective thermo-mechanical parameter in solid geomaterial. In: Advances in Laboratory Testing and Modelling of Soils and Shales, Springer, pp 85–95 *(Cited page 2)*

Xiong MX, Liew JR (2016) Mechanical behaviour of ultra-high strength concrete at elevated temperatures and fire resistance of ultra-high strength concrete filled steel tubes. Materials & Design 104:414–427 *(Cited pages 2 and 3)*

Zhang F, Zhao J, Hu D, Skoczylas F, Shao J (2018) Laboratory investigation on physical and mechanical properties of granite after heating and water-cooling treatment. Rock Mechanics and Rock Engineering 51(3):677–694 *(Cited pages 1 and 3)*

Zhao X, Zhao Z, Guo Z, Cai M, Li X, Li P, Chen L, Wang J (2018) Influence of thermal treatment on the thermal conductivity of beishan granite. Rock Mechanics and Rock Engineering 51(7):2055–2074 *(Cited page 1)*

Zhao Y, Feng Z, Zhao Y, Wan Z (2017) Experimental investigation on thermal cracking, permeability under hthp and application for geothermal mining of hdr. Energy 132:305–314 *(Cited pages 1 and 2)*